A New Technique for Predicting the Shape of Solution-Grown Organic Crystals

Daniel Winn and Michael F. Doherty
Dept. of Chemical Engineering, University of Massachusetts, Amherst, MA 01003

A method for predicting the shape of solution-grown organic crystals is presented. The shapes depend on properties of their internal crystal structure, as well as on the processing environment. The model developed here can account for the effects of solvent and may be extended to account for the influence of certain types of additives. This method may be used as a first approach for including crystal shape in the overall design and optimization of organic solids-processes. The technique has been used successfully to predict the shape of adipic acid grown from water, biphenyl from toluene, and ibuprofen from polar and nonpolar solvents.

Introduction

The shape of crystalline organic solids is an important factor in the design and operation of solid-liquid separation systems. Crystal morphology affects the efficiency of downstream processes (such as filtering, washing, and drying), and influences material properties such as bulk density and mechanical strength which play a major role in storage and handling. It also affects particle flowability, agglomeration, and mixing characteristics, as well as their redissolution properties. Since many organic solids produced in the chemical industry are sold as end-products, the quality and efficacy of these materials also depend in large part on crystal shape. The focus in recent years on specialty chemical processes, like pharmaceuticals, has added to the demand for methods that can predict and control crystal morphology (Davey, 1991; Tanguy and Marchal, 1996).

Since the early days of crystal shape modeling, the primary focus has been the influence of the internal crystal structure on the external crystal habit. Bravais (1866), Friedel (1907), Donnay and Harker (1937), as well as Hartman and Perdok (1955) and others (see the review by Myerson and Gind, 1993), all proposed similar relationships: the greater the surface density of molecules on a face, the stronger the lateral interactions among molecules, and the more stable and slow growing it must be. Thus, low Miller index faces are dense, slow growing, and dominate the crystal shape, as seen experimentally. More recent work in this field has focused on the actual magnitude of interactions within the crystal. The advent of force-fields to calculate van der Waals and electrostatic interactions between organic molecules in the solid state has led to a burgeoning of ideas of how these forces influence morphology. Saska and Myerson (1983) and Berkowitch-Yellen (1985) were among the first to calculate solid-state energies of organic materials for the purpose of morphological modeling. An especially important contribution has been the work of Roberts and co-workers (Docherty and Roberts, 1988a; Clydesdale et al., 1991) who developed the program HABIT, a fast and easy tool for calculating the interaction energy within organic crystals.

The results of this research are models and methods that provide estimates of the relative growth rates of various crystal faces solely from knowledge of the internal crystal structure. Since the construction of the growing crystal polyhedron depends only on relative rates of growth (Hoffman and Cahn, 1972), the crystal shape can be determined. These predictions are often accurate for vapor grown crystals, but are generally not accurate for solution growth. They fail to account for the influence of the crystallizer solution and the driving force (supersaturation) that are widely thought to be major factors affecting shape (Wells, 1946; Myerson and Gind, 1993).

Of the many attempts to account for these factors, the most quantitative success has been achieved by Bennema and coworkers (Liu and Bennema, 1993, 1996; Liu et al., 1995). They have applied the methods of statistical mechanics to examine solvent and supersaturation effects at the crystal-solution interface, and have combined these formulations with detailed growth kinetics—the well known theories of Burton, Cabrera and Frank (1951)—as a means of predicting crystal shape

Correspondence concerning this article should be addressed to M. F. Doherty.

from solution. Their model requires solvent-crystal physical properties that are estimated from detailed experiments or molecular dynamics simulations. This new technique, however, has not yet been widely applied. The need for lengthy simulations or experiments greatly limits its utility for process engineering applications.

We propose a method for predicting crystal shape that can account for realistic processing conditions, and does not necessitate extensive molecular simulation. It is based on similar physical principles to those proposed by Bennema and co-workers (Liu et al., 1995; Liu and Bennema, 1996), but requires only knowledge of pure component properties that, for many systems, are readily available: the crystal structure and internal energy of the solid and the pure component surface free energy of the solvent. Solid–solvent interface properties are estimated using a classical approach that we describe later in the article.

The simplicity and ease of the method permits its use during the discovery stage of an organic solids process (such as to guide experiments). In addition, it may be advantageous to include this shape calculation, along with the traditional predictions for crystal size and size distribution in the overall flowsheet design and optimization of these processes.

Thermodynamics of Crystal Surfaces

In a solution crystallizer with seeds or nuclei, a supersaturation causes the transfer of solute from solution onto the surfaces of individual crystals. With the addition of molecules onto a macroscopically flat crystal surface (a crystal face), there is a change in the Gibbs free energy (kJ/mol) (at fixed T and P) of the entire system corresponding to

$$\Delta G = -N\Delta\mu + \gamma A \tag{1}$$

where $\Delta\mu = \mu - \mu_{sat}$, the difference between the chemical potentials of the solute in solution and in the crystal phase (in units of energy per mole), N is the number of moles transferred, γ is the specific surface free energy (erg/cm^2), and A is the area of the new surface that is formed. The first term represents a decrease in free energy due to a phase change, and the second term represents an increase in free energy due to surface formation. The new surface is an edge surface, a surface of monolayer height wrapping around a molecule, or cluster of molecules. To indicate this, we will write γ as γ^{edge}.

Equation 1 can be used to examine the free energy change associated with one individual cluster of molecules, termed a two-dimensional (2-D) nucleus. To a first approximation, the 2-D nucleus is a disc with an isotropic γ^{edge}, a volume of $\pi r^2 d$ and an edge area of $2\pi rd$, where d is the interlayer spacing (Å) of the given face (see Figure 1). Since N is the volume divided by the molar volume V_M (cm^3/mol) ΔG is a function of r as given by (unit conversion factors are omitted for clarity)

$$\Delta G = -\pi r^2 d\frac{\Delta\mu}{V_M} + 2\pi rd\gamma^{edge} \tag{2}$$

At low supersaturations and $\gamma^{edge} > 0$, the free energy change is positive and increases with r. However, at a certain

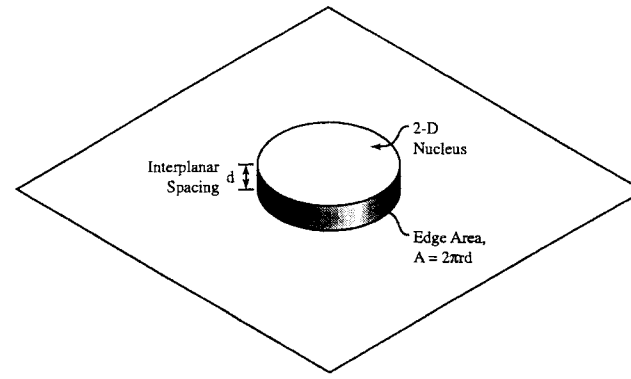

Figure 1. Circular 2-D nucleus on a crystal face.

critical size, ΔG reaches a maximum; the critical radius at which this occurs is given by

$$r_c = \frac{\gamma^{edge}V_M}{\Delta\mu} \tag{3}$$

A nucleus of a size equal to r_c is in unstable equilibrium: smaller ones redissolve; larger ones grow. The change in free energy associated with the creation of one nucleus of critical size is

$$\Delta G_c = \frac{\pi(\gamma^{edge})^2 V_M d}{\Delta\mu} \tag{4}$$

Note that when the supersaturation is high, the critical size can be very small, down to a minimum of one molecule.

Similar equations can be developed for nuclei of other shapes. For example, with a square nucleus of dimensions l by l, Eq. 3 and Eq. 4 become

$$l_c = \frac{2\gamma^{edge}V_M}{\Delta\mu} \tag{5}$$

$$\Delta G_c = \frac{4(\gamma^{edge})^2 V_M d}{\Delta\mu} \tag{6}$$

The general formula for a regular n-sided nucleus is

$$l_c = 2\tan(\pi/n)\frac{\gamma^{edge}V_M}{\Delta\mu} \tag{7}$$

$$\Delta G_c = n\tan(\pi/n)\frac{(\gamma^{edge})^2 V_M d}{\Delta\mu} \tag{8}$$

The free energy change can be expressed in units per mole of critical nuclei by multiplying Eq. 8 by Avogadro's number. It can then be simplified by defining an edge free energy per mole of edge molecules

$$\phi^{edge} = \gamma^{edge}A_M^{edge} \tag{9}$$

where A_M^{edge} is the area (cm^2/mol of edge molecules). Since

$(A_M^{edge})^2 = N_A V_M d$, the free energy per mole of critical nuclei can be expressed as

$$\Delta G_c = n \tan(\pi/n) \frac{(\phi^{edge})^2}{\Delta\mu} \tag{10}$$

This equation will be used later in the article as part of models for predicting the growth rates of crystal faces.

The concept described above—the existence of a maximum in the free energy change as a 2-D nucleus increases in size—is applicable primarily to nuclei on low index crystal faces. Since the operating strategy in many crystallization processes is to maintain a relatively constant supersaturation within the metastable zone, the existence of a physically meaningful maximum (larger than one molecule) depends on γ^{edge} being an adequately large, positive value. Nuclei on low index faces have, in general, a large edge free energy due to a large loss of lateral solid–solid intermolecular interactions at the edges (an increase in internal energy at the edges). On high index faces, however, there are usually fewer and weaker lateral interactions, and γ^{edge} can be very small. Under realistic supersaturations, the above equations could yield a critical radius that is smaller than one molecule. The physical interpretation is that the existence of individual molecules dispersed on these faces lowers the free energy of the system. Such faces tend to roughen, losing their distinct orientation, and develop an interfacial region which is a mixture of solid and ambient-phase molecules. If the ambient phase is a solvent, especially one that is chemically similar to the solid, it can contribute to this phenomena by interacting with edges in a fashion which lowers γ^{edge}. [If the ambient phase is chemically dissimilar to the solid (such as polar solvent/nonpolar solid), then it might have the opposite effect. It may increase edge free energies, and favor the formation of flat faces.]

There is another major influence favoring this *surface roughening* phenomena. Both Burton et al. (1951) and Jackson (1958) showed that the formation of more than one nucleus leads to cooperative effects, and that there can be a substantial increase in the configurational entropy of the system when multiple nuclei are dispersed on a face. In effect, γ^{edge} is not just a function of internal energy (the unsaturated interactions of nuclei), but also depends on the number, size, and configuration of nuclei. If the internal energy effects are small enough, it is possible for the configurational effects to dominate, and even with no supersaturation, a rearrangement to a rough interface can be favorable (γ^{edge} is effectively zero). This is generally referred to as *thermodynamic roughening.* In the case where configurational effects do not dominate internal energy effects (γ^{edge} is a small, positive value), then the face is rough only above some critical supersaturation (Bennema, 1993). This is termed *kinetic roughening.*

Growth Kinetics

For faces that are rough, there are no energetic barriers associated with incorporating material into the crystal surface. Thus, growth in these directions is diffusion and/or heat-transfer limited. Since these processes are relatively isotropic, rough faces tend to lose their distinct orientation. Evidence from crystal growth simulations (Gilmer and Bennema, 1972), as well as from experiments (Hunan et al., 1981; Jetten et al., 1984), indicate that rough faces grow an order of magnitude faster than the slowest flat faces on a crystal.

The growth of flat faces is thought to occur by the movement of monolayer steps. Material is added to steps that propagate laterally and spread out over a face. Each complete layer results in the advancement of the face by a distance of monolayer height in the direction of the surface normal. Very convincing evidence of this mechanism can be seen in recent *in-situ* atomic force microscopy (AFM) studies of organic crystal growth (Manne et al., 1993; Carter et al., 1994; Yip and Ward, 1996).

Growth by steps requires the formation of a stepped interface, as well as the desolvation, transport, and incorporation of material into the step. One possible source of steps are 2-D nuclei; the edge of the nucleus creates a step perpendicular to the face. Several authors (Lewis, 1974; Ohara and Reid, 1973; Chernov, 1984; van der Eerden, 1993; Markov, 1995) present detailed descriptions of growth by 2-D nucleation. The most realistic of these is the so-called birth and spread model (see the figure on p. 37 of Ohara and Reid, 1973). In Markov's (1995) development of 2-D nucleation from solution, the expression for the relative growth rate of faces has a proportional dependence on two functions: $\exp(-\Delta G_c/3RT)$, and $\exp(-U/RT)$, where U is the desolvation activation energy (kJ/mol). As discussed in the Appendix, it can be shown that faces with the large ΔG_c also have a small U, and vice versa; they vary inversely, but not proportionally. The velocity of a face decreases with increasing ΔG_c, but not by an exponential dependence. We, therefore, propose as an approximation that the relative growth rate follows an inverse proportionality dependence, and, thus, the expression

$$R_{rel} \propto \frac{1}{\Delta G_c} \tag{11}$$

The range of applicability is the same as in the original model, that is, $\Delta G_c > 3RT$. When ΔG_c approaches $3RT$, the face becomes roughened by the presence of many nuclei, and growth no longer proceeds by a stable, flat growth mechanism (van der Eerden, 1993).

When $\Delta G_c \gg 3RT$, as is the case when γ^{edge} is large and $\Delta\mu$ is small, growth by a 2-D nucleation mechanism is extremely slow. Burton, Cabrera and Frank [BCF] (1951), in their seminal article, suggested that there must be another source of steps if growth was to proceed under these conditions. They suggested that screw dislocations on crystal faces provide an infinite source of steps. The edge from a screw dislocation grows laterally and rotates about itself, resulting in a *growth spiral* of steps (see Figure 2). Once a moving step has reached the initial position of the directly underlying step, the spiral has made a complete turn. This rotation increases the height of the spiral, causing the macroscopic face to advance. The BCF expression for the rate of growth of a face is thus

$$R_{rel} = \frac{d \times v}{y} \tag{12}$$

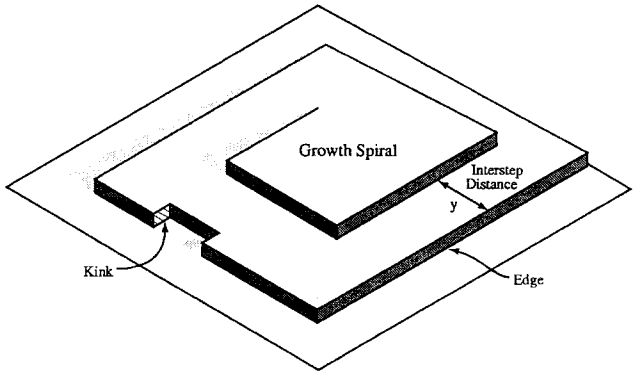

Figure 2. Square spiral originating from a screw dislocation on a crystal face.

where d is the step height, v is the lateral velocity of the step, and y is the lateral distance between steps. In the limiting case where (1) we ignore bulk or surface diffusion effects (as argued by Chernov (1984) for solution growth), and (2) we assume that steric barriers are isotropic, then the face dependent portion of the step velocity depends mainly on the density of *kink sites* (vacancies in the step where material can incorporate) multiplied by the distance the step is propagated

$$v \propto a_p[1+0.5\exp(\phi^{\text{kink}}/RT)]^{-1} \tag{13}$$

where a_p is the distance (Å) that edge is propagated by adding a monolayer to it; the term in brackets is the probability of finding a kink in a step at equilibrium, and ϕ^{kink} is the work, or free energy change, to create a kink along an edge (Burton et al., 1951). Therefore, with only face dependent parameters, Eq. 12 becomes

$$R_{\text{rel}} \propto \frac{d}{y} a_p[1+0.5\exp(\phi^{\text{kink}}/RT)]^{-1} \tag{14}$$

This expression remains valid only when ϕ^{kink} is greater than RT (Burton et al., 1951). When it is smaller, kinks are sufficiently numerous that edges are roughened, and edge free energy is sufficiently low that 2-D nucleation occurs.

Kink free energy can also be defined as

$$\phi^{\text{kink}} = \gamma^{\text{kink}} A^{\text{kink}} \tag{15}$$

where γ^{kink} is the free energy of forming a kink per unit kink area, and A^{kink} is the kink area (cm^2/mol).

The general formula for the interstep spacing is $y \propto \kappa\gamma^{\text{edge}}$, where κ depends on the geometry of the spiral. In the next section, we derive this relationship and give explicit values for κ. In addition, since $\phi^{\text{edge}} = A_M^{\text{edge}}$, and since $A_M^{\text{edge}} \times a_p = V_M = \text{constant}$, Eq. 14 reduces to

$$R_{\text{rel}} \propto \frac{d}{\kappa\phi^{\text{edge}}}[1+0.5\exp(\phi^{\text{kink}}/RT)]^{-1} \tag{16}$$

We now have two expressions for the relative rates of growth of crystal faces: Eq. 16, the screw dislocation model, when $\phi^{\text{kink}} > RT$; and Eq. 11, the 2-D nucleation model, which might occur when $\phi^{\text{kink}} < RT$. We cannot be certain of 2-D nucleation when $\phi^{\text{kink}} < RT$, since it is possible that spiral growth occurs without any kink integration limitations (that is, by mass-transfer limited spiral growth). A comparison between these two possibilities requires calculating *absolute* growth rates, which are a function of supersaturation as well as transport and molecular properties (such as vibrational frequencies). Since one cannot, in practice, calculate these absolute growth rates, we will make the assumption that $\phi^{\text{kink}} < RT$ results in 2-D nucleated growth. Under this low kink energy regime, we can also apply the condition that faces with $\Delta G_c < 3RT$ are rough and grow by a fast/diffusion limited mechanism. Thus, we distinguish three growth regimes, all of which are a function of the face-dependent parameters ϕ^{edge} and ϕ^{kink}. In a later section we describe methods for estimating their values.

Spiral geometry

The geometry of a growth spiral originates in the work of BCF with further developments by Cabrera and Levine (1956). An excellent summary of their work can be found in the review of Ohara and Reid (1973). In these early developments, the spiral is thought to be circular with numerous kinks, and its edge velocity is assumed to be surface-diffusion-limited. Kaichew (1962) and Voronkov (1973) examined the geometry of spirals with straight edges and few kinks—a low temperature/high kink energy regime—where the edge velocity is limited by kink integration kinetics. Muller-Krumbhaar (1978) performed Monte Carlo simulations of spiral crystal growth under both regimes, with results that are consistent with these original theoretical developments. Since the model developed above for solution growth assumes only kink integration kinetics, we will focus on the physics of faceted spirals formed from completely straight (or approximately straight) edges.

The basic principle governing spiral motion is that the very top of a rotating spiral is stationary. Since a 2-D layer that neither grows nor dissolves is of critical size, the very top edge of the spiral must be of critical length. Thus, $v = 0$ for $l \le l_c$. The velocity of edges greater than l_c depends on the growth mechanism; for our case, velocity depends on the kink density. In Eq. 13, we presented an expression for the equilibrium kink density, and it is not a function of the edge length. Thus, we would expect that any edge on a spiral with a length greater than l_c will travel at its steady-state velocity. Voronkov (1973) has presented a nonequilibrium derivation of kink density, and has also determined that kink density is not a strong function of edge length. It is, therefore, reasonable to assume that all edges greater than l_c have the same density of kinks. The edge velocity can be expressed as

$$\begin{aligned} v &= 0, \quad && l \le l_c \\ v &= v(\text{eq}), && l > l_c \end{aligned} \tag{17}$$

where v(eq) is just the velocity of the straight edge with its equilibrium concentration of kinks as given by Eq. 13.

One must also consider which, and how many, straight edges are likely to appear on a growth spiral. Since the maximum rotational symmetry in a 2-D lattice is six, there cannot

be an n-sided spiral, with $n > 6$, such that all edges have the same molecular density and bonding. All n-sided $n > 6$ spirals have all of the most densely packed edges with high kink energies and slow growth, and additional edges that are less dense and faster growing. It is reasonable to assume that only the most dense, slowest growing edges dominate the spiral shape, and this reduces the number of spiral facets to a number no greater than six. As we will discuss in detail in a later section, the most dense edges dominating spiral shape are those that contain first nearest neighbor interactions.

We can determine the number of possible first nearest neighbor interactions by examining the packing arrangement of molecules in two dimensions. Only five lattices are possible: square, rectangular, centered rectangular, oblique, and hexagonal (Giacovazzo, 1992). It is trivial to show that for all these arrangements, it is only possible to have one, two or three edge directions with first nearest neighbors. When a face contains two edges with first nearest neighbors, the spiral is four-sided. (It can be exactly square if it stems from square packing; it can be thought of as quasi-square if it stems from oblique packing). When there is only one edge with first nearest neighbors, this slow growing edge is much larger in size than the other fast growing, less dense edges—the spiral is very elongated and can be thought of as rectangular. If there are three edges with first nearest neighbors, then the spiral is six-sided. Thus, under our first nearest neighbor/kink integration limited assumptions, there exists only these limited spiral shapes.

Kaichew (1962) employed the principles of Eq. 17 to estimate the interstep distance in the case of a square spiral: a four-sided spiral with identical bonding structure in the two edge directions, and thus the same values of v and γ^{edge} in both edge directions. In this construction, growth begins from an initial edge dislocation. The entire edge moves forward a distance infinitesimally greater than l_c, so as to create a new edge, perpendicular to it, of length infinitesimally greater than l_c. This new edge can now grow at its steady-state velocity, and it repeats the same movement. Four such motions are required to form a complete spiral. During this time, the initial edge has moved forward a total of $4l_c$, and, thus, the distance between steps is $4l_c$. Given l_c from Eq. 5, the interstep distance is proportional to $8\gamma^{\text{edge}}$ ($\kappa = 8$).

We might also consider the case where, due to asymmetry in the molecules and chemical interactions, the two dense edges have small differences in their energetic properties. The result is a situation where γ^{edge} and ϕ^{kink} vary only slightly in the two edge directions, while the velocity varies more substantially because of the exponential dependence in Eq. 13. Using subscripts i and j to denote the two edge directions, i being the slower of the two, the spiral construction yields an interstep distance given by

$$y_i \propto \left(4 + \frac{4}{v_j/v_i}\right)\gamma^{\text{edge}} \tag{18}$$

where $v_j \geq v_i$, and where we have assumed that γ^{edge} remains essentially independent of edge direction.

Equation 18 allows us to make an estimate of y_i in the case of only one stable, slow growing edge on a face. When the fast growth directions can be approximated by one principal fast direction j that is perpendicular to the stable edge ($v_j \gg v_i$), the interstep spacing becomes

$$y_i \propto 4\gamma^{\text{edge}} \tag{19}$$

The six-sided spiral can be constructed in the same manner as the Kaichew construction (Voronkov, 1973). In this case, the initial edge moves forward six times during a complete rotation. Each movement is a distance $l_c \sin(2\pi/6)$. Substituting l_c from Eq. 7, the interstep distance is proportional to $6\gamma^{\text{edge}}$ ($\kappa = 6$). If there are differences in the velocities of the three directions, the interstep distance can be calculated in a manner analogous to Eq. 18

$$y_i \propto \left(2 + \frac{2}{v_j/v_i} + \frac{2}{v_k/v_i}\right)\gamma^{edge} \tag{20}$$

where v_j and v_k are the two faster growing edges.

The pre-factors of γ^{edge} in Eqs. 18 through 20 are the κ values necessary for application of the spiral growth model.

Estimating Physical Properties

The development thus far presents ϕ^{edge} and ϕ^{kink} as the key solvent-dependent physical properties affecting crystal shape. Their values can be derived from γ^{edge} and γ^{kink}. The former is an interfacial property in the classical sense; microscopy has shown that edges on crystal faces delineate a distinct boundary between the crystal and ambient phases. On the other hand, because a kink is of molecular dimensions it is not an interface on a macroscopic scale. Nevertheless, in order to develop a first-order estimation of γ^{kink} we assume that the free energy to form a kink can be approximated by an effective interfacial free energy for the formation of a 2-D interface separating the solvent and solid at kink sites.

There are several potential approaches for obtaining values of interfacial thermodynamic quantities: experimental measurements, molecular level simulations, group contribution estimations, and so on. The first approach is not feasible, because it is not possible to measure interfacial free energy at molecular-sized interfaces. Molecular modeling at the organic solid-solution interface is feasible, and has recently been employed for morphological modeling purposes (Boek et al., 1994). The main drawback of this approach is the large computational time required to simulate the solution in contact with many edges on many faces. For purposes of process engineering, this method does not yet seem efficient; however, with advances in computing and in computational chemistry, it may soon become the desirable approach. A group contribution method would also be extremely useful, although no precise methods exist for organic interfacial systems.

We, therefore, employ a simple classical approach for estimating interfacial properties, one first suggested in the work of Hildebrand on the thermodynamics of mixing (see Hildebrand and Scott, 1962), and later fully developed by Girifalco and Good (1957). The formation of an interface at equilibrium between two phases is thought of as a three-stage process: creating a surface between the first phase and a vacuum, creating a surface between the second phase and a vac-

uum, then bringing the two surfaces into contact. The first two steps result in a free energy increase, often termed the free energy of *cohesion* (for each surface). The third step causes a free energy decrease which is often termed the free energy of *adhesion*. The development of Girifalco and Good suggests that the free energy of adhesion per unit area can be approximated by twice the geometric mean of the two cohesive surface free energies. Thus, the net free energy per area of an interface between phase α and phase β can be written as

$$\gamma^{\alpha,\beta} = \gamma^{\alpha} + \gamma^{\beta} - 2\sqrt{\gamma^{\alpha}\gamma^{\beta}} \tag{21}$$

This representation is often referred to as the *geometric mean approximation*. Its physical premise is analogous to that of the regular solution model of mixing, and, thus, it is most valid when the surface enthalpy can be approximated by the surface energy, and the net change in entropy for interface formation is zero (or $T = 0$). It also holds approximately true if the change in entropy at the interface also follows the geometric mean rule. Equation 21 tends to match experimental results for solution–solution interfacial free energy, where γ^{α} and γ^{β} are taken from measured surface tensions in contact with air (Barton, 1983).

Equation 21 can be further extended to the case where one of the phases has some electrostatic or polar component to its surface free energy. [We define electrostatic component of the free energy in the way normally prescribed in solubility parameter theory for internal energy; that is, some portion of the total free energy stems from dispersive forces, and the rest—the electrostatic component—is due to dipole-dipole and/or hydrogen bonding. The division of free energy in this way is not on as firm a theoretical footing as when it is applied to internal energy only. However, because surface free energy tends to correlate with the bulk internal energy (Barton, 1983), it is suspected that surface entropy does correlate with the amount and type of forces contributing to the internal energy.] If we assume that there are no induced electrostatic interactions in the free energy of adhesion, then Eq. 21 can be rewritten as

$$\gamma^{\alpha,\beta} = \gamma^{\alpha} + \gamma^{\beta} - 2\sqrt{\gamma^{\alpha}\gamma'^{\beta}} \tag{22}$$

where the prime symbol denotes only the dispersive (van der Waals) component of the surface free energy.

Writing this relationship for the effective interfacial free energy at a kink

$$\gamma_i^{\text{kink}} = \gamma_i^{\text{cryst}} + \gamma^{\text{solv}} - 2\sqrt{\gamma_i^{\text{cryst}}\gamma'^{\text{solv}}} \tag{23}$$

where the superscripts denote crystal and solvent phase surface free energies, and the subscript i denotes a kink site on a particular edge on a crystal face.

In writing Eq. 23, we have allowed the solvent to be polar or nonpolar, while we have explicitly restricted the solid–solid interactions to dispersive forces only. Thus, its range of applicability is somewhat limited. However, the forces within organic crystals are often dominated by dispersive forces, while the electrostatic contributions are mostly limited to a few specific interactions, usually hydrogen bonds. Thus, Eq. 23 can be applied to all kink interfaces, except those that are formed by these specific electrostatic bonds. For these kinks, we can approximate the interfacial free energy with experimental measurements of liquid–liquid interfacial free energies of substances of a similar chemical nature (available in the literature). A common situation is when the solvent is highly polar (such as water), and a crystal kink surface is dominated by unsaturated hydrogen bonds (such as carboxyl groups). For such cases, γ^{kink} should be quite small. Faces with these kinks should have high kink densities and fast growth, and the overall crystal morphology will not be sensitive to this approximation.

Another restriction on the application of the geometric mean approximation to surface free energy is that it is most accurate when the intermolecular distance at the interface (that is, normal to the interface) is close in magnitude to the intermolecular distances of the two individual phases (Girifalco and Good, 1957). It is often the case in organic crystallization that the solute has a larger molecular volume than the solvent; thus, we expect that crystal edges formed from the most dense chains of molecules (smallest intermolecular distances) are those that are closest in molecular dimension to the solvent. These are the edges to which Eqs. 22 and 23 can be applied. The other less dense edges generally do not appear on the surface structures, and, thus, their exact interface properties are not needed for morphological prediction. Their large intermolecular spacing results in weak solid–solid bonding (low kink energies and high kink densities), and also reduces steric barriers to mutual dissolution (the edge may be "porous"with respect to the solvent). These edges are disordered and fast growing with disordering analogous to surface roughening discussed earlier.

Although the theoretical aspects of edge roughening have been discussed by several authors (see the review by Chernov and Nishinaga (1987)), the effect cannot be captured quantitatively without a means for predicting kink energies on the less dense edges. However, some insight can be gathered from molecular simulations of ideal Kossel, cubic packed crystals (Muller-Krumbhaar, 1978; Markov, 1995). These studies have been able to successfully predict physical phenomena (such as face roughening and spiral geometry) when assuming that only first nearest neighbor interactions affect surface structure. All longer-distance interactions are assumed *a priori* to result in rough, unstable, and fast growing edges. We propose using this same assumption to determine the likely stable edges within solution grown crystals. A strict definition of nearest neighbor is "a molecule whose center of mass is within the first coordination sphere of a central molecule's." For crystals with mainly dispersive forces between molecules, this coordination sphere can be defined by the material's characteristic packing diameter

$$D_m = 2\left(V_m \frac{3}{4\pi}\right)^{1/3} \tag{24}$$

where V_m is the molecular volume (Å^3). Any chain of molecules within the crystal whose intermolecular distance l_i (Å) is within a distance D_m is considered to have nearest neighbor interactions. We can state this criterion as

$$l_i \le D_m \tag{25}$$

Edges that satisfy the criterion are thought to be reasonably stable, have similar bonding distances to those in the solvent, and, thus, have kink interfaces to which Eq. 23 can be applied.

For crystals that contain chains of hydrogen bonds, the packing motif is a function of the dispersive forces between these chains. Therefore, the diameter characteristic of dispersive forces is defined by $D_m = 2(A_{hkl}^{\max}/\pi)^{0.5}$, where $A_{hkl}^{\max}$ is the reticular density of the most dense face intersected by the chains. For crystals that contain 2-D layers of hydrogen bonds, the characteristic diameter is the distance between adjacent layers. Some of the intermolecular interactions in a crystal that do not satisfy the criterion (that is, $l_i > D_m$) may nevertheless have dispersive energies greater than or equal to those that do (a result of the molecular asymmetry). We must assume that such interactions are first nearest neighbors as well. We will also include hydrogen bonds as first nearest neighbors, since they are by definition short-range interactions between adjacent molecules.

The remaining unknown parameter in this morphological model is edge free energy. Liu and Bennema (1996) have shown that on a square nucleus, the kink surface in one edge direction is the edge surface of the other direction. Thus, $\gamma_j^{\text{edge}} = \gamma_i^{\text{kink}}$ where i and j are the two edge directions. Since we assume in the 2-D nucleation model that the nuclei are isotropic—that they are not the Wulff shape, but a cluster that is dominated by the relatively isotropic packing and bonding properties in the solid—then we can define an average γ^{edge} for the nucleus. Therefore, on a given face

$$\gamma^{\text{edge}} \approx \bar{\gamma}^{\text{kink}} \tag{26}$$

where $\bar{\gamma}^{\text{kink}}$ is the mean of all γ_i^{kink} on a given face. This average value can be used in the spiral growth formalism, since the rate expression is a much stronger function of edge velocity than of edge free energy. A further approximation which simplifies the calculation for a square nucleus is

$$\phi^{\text{edge}} \approx \bar{\phi}^{\text{kink}} \tag{27}$$

A kink surface does not correspond to an edge surface on a six-sided nucleus or spiral. Hexagonal packing results in edges that have two unsaturated solid–solid contacts. Thus, we approximate the edge free energy by

$$\phi^{\text{edge}} \approx 2\bar{\phi}^{\text{kink}} \tag{28}$$

A difficulty in estimating edge free energy arises when Eq. 25 yields only one first nearest neighbor edge direction on a face. We have assumed that all other edge directions on the face are rough. In the case where the "stable" edge itself has a low kink free energy (less than RT), all edge directions are rough and the 2-D nucleation mechanism is applied (see the growth kinetics section). The nucleus can be pictured as a relatively isotropic disk dominated by two rough growth fronts: one in the direction of the "stable" edge, and the other which we assume is approximately perpendicular to it. (The nucleus is quasi-square with rough edges). Since the "stable" edge has a very low ϕ^{kink}, the rough growth front is not likely to have a ϕ^{kink} significantly greater than zero. We can roughly estimate the edge free energy as the average of the one calculated ϕ^{kink}, and zero

$$\phi^{\text{edge}} = \frac{1}{2}\phi^{\text{kink}} \tag{29}$$

In the case where the one stable edge has a large kink free energy, the edge is unroughened, while other edge directions are assumed roughened. We expect that spiral growth occurs, and that the spiral is bounded by the one stable edge and a roughened growth front that is approximately perpendicular to it. Because this growth front has bonding and packing geometry that is not vastly different from the stable edge, we suspect that its kink free energy is as close to the stable edge's value as possible; that is, it has the largest possible ϕ^{kink} that leads to roughening. As mentioned earlier, the theoretical value for this limit is RT, which is approximately 2.5 kJ/mol at room temperature. Thus, the edge free energy can be estimated from the average of the calculated ϕ^{kink} and RT

$$\phi^{\text{edge}} = \frac{1}{2}(\phi^{\text{kink}} + RT) \tag{30}$$

Solvent properties

Solvent surface free energies have been measured for many solvents in contact with air (Adamson, 1990; Kaelble, 1971). In addition, within certain classes of solvents, γ^{solv} correlates with their bulk solubility parameters. [See Barton (1983) for details on solubility parameters, their values, and their correlations to surface properties.] Therefore, unreported solvent surface free energies, as well as the dispersive components of the surface free energy, can be estimated using these relationships.

The empirical correlations in Kaelble (1971) and Barton (1983) have the form

$$\gamma'^{\text{solv}} \approx 0.143\delta_d^2 N_A^{-1/3} V_M^{1/3} \tag{31}$$

where δ_d is the dispersive solubility parameter, N_A is Avogadro's number, and V_M is the molar volume. For example, water at room temperature has a measured γ^{solv} of 72.8 erg/cm^2. Using $\delta_d = 7.6$ (cal/cm^3)$^{1/2}$ (Hansen and Beerbower, 1971) and Eq. 31, we find that γ'^{solv} makes up about 10 erg/cm^2 of the total.

Crystal properties

We assume that changes in internal energy dominate the creation of crystal surfaces in contact with a vacuum. Thus, the surface free energy is approximately equal to the surface energy, which can be estimated from intermolecular forces (Kitaigorodsky, 1973). The calculation of internal energy within crystals and at crystal surfaces has been widely applied using the well known *attachment energy* technique (Saska and Myerson, 1983; Berkovitch-Yellin, 1985; Docherty and Roberts, 1988b; Green et al., 1993), and there are excellent software programs available, most notably HABIT (Clydes-

dale et al., 1991) and Cerius[2]. These programs are fast and easy to use, and require only the crystal structure and choice of force field as input.

The output from these calculations provides a per mole value of the intermolecular energy between a central molecule and every other molecule in the crystal. These molecule–molecule interactions are traditionally referred to as "bond energies" (noncovalent), and have a corresponding bond distance between centers of mass. Because of the repeating nature of the crystal lattice, these bonds form chains running throughout the crystal. If the chain is parallel to a face, it can form the boundary of an edge on that face. Denoting bond energy along an edge i as ϕ_i^{cryst}, bond length by l_i, and an effective kink area of $A_i^{\text{kink}} = V_m/l_i$, we can calculate the effective surface energy at a kink by

$$\gamma_i^{\text{cryst}} = \phi_i^{\text{cryst}}/A_i^{\text{kink}} \tag{32}$$

Note that we only perform this calculation on bond chains that satisfy the criterion of Eq. 25, and with only the dispersive component of the energy.

Likely Crystal Faces

The law of Bravais, Freidel, Donnay and Harker (BFDH) (see the computer implementation of this law, MORANG, by Docherty and Roberts (1988a)) is an efficient means of choosing the likely crystal faces for which one should calculate face growth rates. It states that the larger a face's interplanar spacing (d_{hkl}), the slower its growth and the greater its size. This corresponds with the kinetic models we have presented—faces with larger d_{hkl} have higher densities of molecules, and, therefore, more nearest neighbors, more stable edges, larger γ^{edge}, and slower growth.

It is possible for several crystallographic forms with different interplanar spacings to have identical first nearest neighbor bonding structures—they have identical bond chains defining their edges. Of these forms, we would expect those with larger d_{hkl} to have greater edge surface area, and, thus, slightly larger edge and kink energies. However, our method of estimating these properties is not sensitive to step height. To compensate, we propose choosing the likely faces by the BFDH approach, but for any set of forms with identical stable bond chains, we retain only the face with the largest d_{hkl}.

Model Implementation

(1) Perform a standard *attachment energy* simulation and interplanar spacing calculation on the material of interest. The output yields the likely faces, the intermolecular bond energies and distances, and indicates which bond chains are parallel to individual crystal faces.

(2) Determine which bond chains correspond to stable edges with first nearest neighbors, satisfying Eq. 25.

(3) Refine the list of likely faces by choosing only those with at least one stable edge. For sets of forms with identical stable edges, choose the one with the larger interplanar spacing.

(4) Calculate γ^{kink} for each of these bond chains using Eq. 23. Obtain ϕ^{kink} from Eq. 15 and ϕ^{edge} from Eqs. 27 through 30.

(5) If the largest $\phi^{\text{kink}} \le RT$, apply the 2-D nucleation model. For each likely face:

- Calculate ΔG_c using Eq. 10.
- Calculate the relative growth rate by Eq. 11. For those faces that are rough due to $\Delta G_c \le 3RT$, the growth rate can be estimated as an order of magnitude (ten times) faster than the average of the unroughened face growth rates.

(6) If the largest $\phi^{\text{kink}} \ge RT$, apply the screw dislocation model. For each likely face:

- Calculate relative growth rate with Eq. 16. Use largest ϕ_i^{kink} on the face, and the corresponding κ from Eqs. 18 through 20 (that is, single edge, square spiral, or hexagonal spiral).

From the relative growth rates, a shape can be drawn using the Wulff construction (Hoffmann and Cahn, 1972). Note that if the flat, slow growing faces intersect only two crystallographic axes, there is rough growth in the direction of the third axis, and the resulting crystal is an elongated needle shape. If the slow growing faces intersect only one principal axis, then the crystal is a thin flat plate.

Example: Adipic acid in water

The shape of adipic acid crystals has been studied extensively with particular interest in improving the acid's flowability (Klug and van Mil, 1994) and its role in pill formation of pharmaceutical compounds (Grant et al., 1991). It is usually crystallized from aqueous solution into a flat plate with large {100} faces bordered by small {011}, {11$\bar{1}$}, {002}, and {10$\bar{2}$} faces. Electron micrographs of adipic acid grown from aqueous solutions in a fluidized-bed crystallizer just below a saturation temperature of 303 K are presented in Figure 3. Experimental details are given in Winn (in press).

Attachment energy and BFDH calculations have been previously performed by Davey et al. (1992), and we have re-

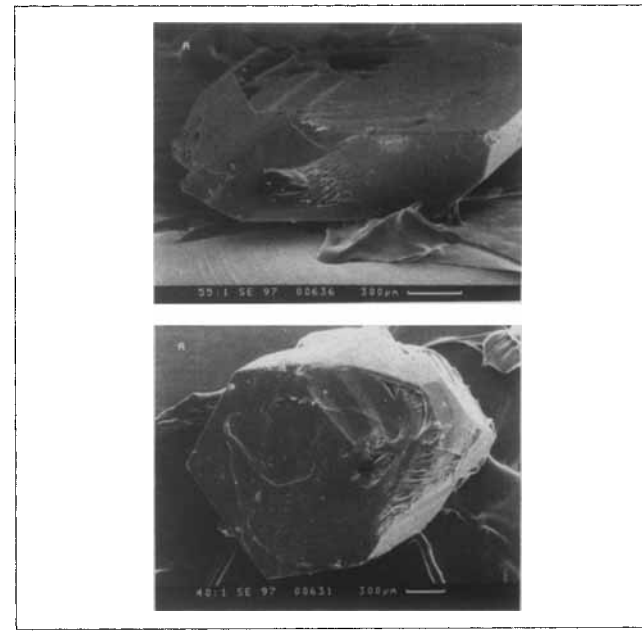

Figure 3. Two views of an adipic acid crystal grown from aqueous solution.

Table 1. Estimated Interfacial Free Energies (Crystal–Water) in the First Nearest Neighbor Bond Chains of Adipic Acid

Label	ϕ^{cryst} (kJ/mol)	l (Å)	γ^{cryst} (erg/cm^2)	γ^{kink} (erg/cm^2)	ϕ^{kink} (kJ/mol)
i, i^*	8.263	5.65	43.26	74.46	14.2
j	7.272	5.15	34.70	70.25	14.7
h		10.1		7.0	0.75

peated these calculations in order to obtain the detailed simulation output (Winn, in press). The three bond chains that satisfy Eq. 25, along with a hydrogen bonded chain are reported in Table 1 with their magnitude and bond distance. The bonds labeled i, i^* (these two are related by symmetry), and j are formed primarily from dispersive forces, while h designates the hydrogen bond. The top eight likely faces from the BFDH model are listed in Table 2. For each, we have listed the bond chains that are coplanar and form stable edges.

Table 1 also contains the results of the physical property predictions: γ^{cryst} from the attachment energy simulation, and, using water surface properties given earlier, the calculated γ^{kink} and ϕ^{kink} values. The value of γ_h^{kink} was taken from a measurement of interfacial free energy of water on liquid heptanoic acid (Girifalco and Good, 1957), and is very small as expected.

The large kink free energy values imply the screw dislocation mechanism. Relative growth rates were calculated, recalling that three edges form a six-sided spiral, and two edges a four-sided one. For the forms with identical sets of stable edges, we included only the one with the larger interplanar spacing. The predicted shape is reported in Figure 4. It is in excellent agreement with the experimental shape, with a similarly large {100} form and an aspect ratio of about four. All of the predicted faces and their relative sizes closely match experimental results of other authors (Davey et al., 1992; Klug and van Mil, 1994). The success of this calculation suggests that the use of an estimate for the hydrogen bond interface property is valid—this has been confirmed with a successful prediction of water grown succinic acid crystal shape (Winn, in press).

Example: Ibuprofen from polar and nonpolar solvents

The importance of ibuprofen's crystal shape to its processing and product quality has been discussed by Gordon and

Table 2. Major Faces of Adipic Acid Ranked by Interplanar Spacing.*

Face	d_{hkl} (Å)	Bond Chains	R_{rel}
100	6.920	i, i^*, j	1.00
$10\bar{2}$	4.768	j	3.04
$20\bar{2}$	4.685	j	
$11\bar{1}$	4.513	i	3.61
011	4.126	i, h	3.69
$2\bar{1}\,\bar{1}$	3.509	i	
002	3.446	j, h	2.45
$30\bar{2}$	3.354	j	

*Along with their stable bond chains and the scaled relative velocities calculated using the spiral growth mechanism.

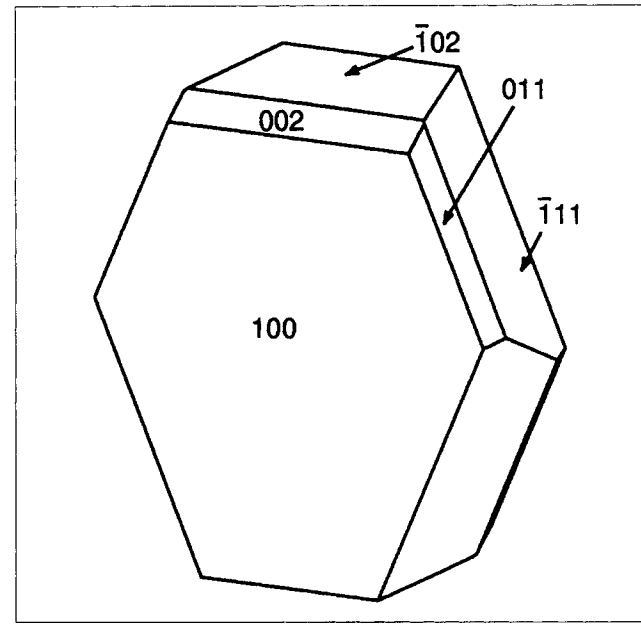

Figure 4. Predicted morphology of adipic acid grown in water.

Amin (1984). The primary interest in this system is the existence of high aspect ratio needles along the b axis when grown from a nonpolar hydrocarbon—usually hexane or heptane—while equant low aspect ratio crystals are formed when grown from polar solvents such as ethanol and methanol. This was discovered by researchers at the Upjohn Company (Gordon and Amin, 1984), who patented the change in solvent as a process improvement. The effect can be seen graphically in Figure 5, where aspect ratio of ibuprofen crystals is plotted vs. the solvent type, which is represented by its hydrogen bonding solubility parameter.

An attachment energy calculation has been performed by Bunyan et al. (1991), using individual molecules as growth units. We have implemented a similar simulation assuming ibuprofen dimer as the growth unit (Winn, in press), and will use these results as input to the solution-growth model. The

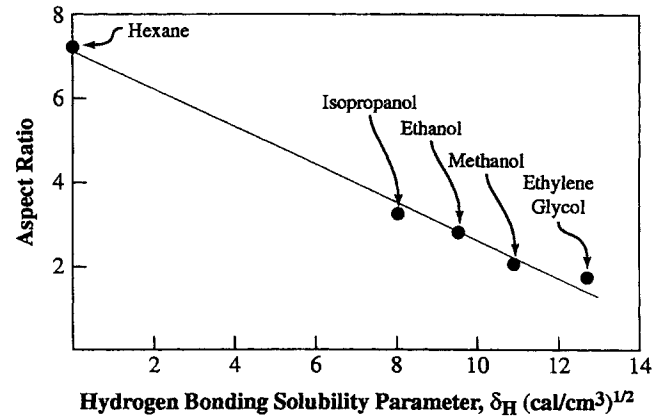

Figure 5. Effect of solvent type on the aspect ratio of ibuprofen crystals

Redrawn from Gordon and Amin (1984).

Table 3. Estimated Interface Properties for Ibuprofen Crystals in Hexane

Label	ϕ^{cryst} (kJ/mol)	l (Å)	γ^{cryst} (erg/cm^2)	γ^{kink} (erg/cm^2)	ϕ^{kink} (kJ/mol)
i	18.234	7.89	39.03	2.43	1.13
j, j^*	15.418	6.66	27.86	0.35	0.19

crystal structure of ibuprofen, like most monocarboxylic acids, is an arrangement of hydrogen-bonded dimers interacting with mainly dispersive forces. It is thought that this packing stems from dimer formation in solution prior to incorporation into the crystal (Gavezzotti et al., 1997).

The morphological model was implemented for two representative solvents: hexane and ethanol. For hexane, $\gamma^{solv} = 22$ erg/cm^2 (Kaelble, 1971). For ethanol, $\gamma^{solv} = 22.8$ erg/cm^2, and using solubility parameters from Barton (1983), we have calculated $\gamma^{solv} = 16.3$ erg/cm^2. The results of implementing the model are given in Tables 3, 4, and 5.

Growth from hexane results in low kink free energies and, thus, we apply the 2-D nucleation model. It is noteworthy that ϕ_j^{kink} is small (0.35 kJ/mol), and we might expect roughening on {011} depending on the supersaturation. The model predicts $\Delta G_c < 3RT$ for {011} when the relative supersaturation is 0.0019 or greater (assuming $T = 313$ K). while the other two forms {100} and {002} remain stable. (Note that we use $\Delta\mu = RT \ln(1+\alpha)$, where α is the relative supersaturation. The relative supersaturation is normally the relative difference in equilibrium activities or, as an approximation, equilibrium concentrations.) We therefore expect rough, fast growth down the b axis at moderate supersaturations. Needle shapes are predicted, which is in agreement with the patent.

For growth from ethanol, we apply the screw dislocation model which results in an equant shape with an aspect ratio of about two. Comparison with Figure 5 (ethanol hydrogen bond solubility parameter is 9.5) indicates that our prediction is again in agreement with the patent. The shapes of both predictions are drawn in Figure 6. The hexane is constructed assuming that the rough growth of {011} is an order of magnitude (ten) times the average growth rate of the two unroughened, slow faces. These calculated morphologies are also very similar to experimental ones reported by Bunyan et al. (1991).

Example: biphenyl grown from toluene

This solute and solvent system are of a similar chemical nature, which should result in low kink and edge free energies, and, thus, 2-D nucleated growth. In addition, we might expect face roughening to occur, even for low index faces. Jetten et al. (1984) have determined experimentally that a transition from flat to rough growth occurs on the {110} faces of biphenyl in toluene when the relative supersaturation is

Table 4. Estimated Interface Properties for Ibuprofen Crystals in Ethanol

Label	ϕ^{cryst} (kJ/mol)	l (Å)	γ^{cryst} (erg/cm^2)	γ^{kink} (erg/cm^2)	ϕ^{kink} (kJ/mol)
i	18.234	7.89	39.03	11.37	5.31
j, j^*	15.418	6.66	27.86	8.02	4.44

Table 5. Predicted Relative Growth Rates on Ibuprofen Crystals Grown from Hexane and Ethanol

Face	d_{hkl} (Å)	Bond Chains	R_{rel} (Hexane)	R_{rel} (Ethanol)
100	14.742	i, j, j^*	1.00	1.00
011	6.324	j	rough	1.96
$11\bar{1}$	6.014	j		
$1\bar{1}1$	5.599	j		
002	5.294	i	2.75	1.13
$10\bar{2}$	5.255	i		
$2\bar{1}\,\bar{1}$	5.509	j		
102	4.729	i		

0.007 (from a saturated solution at 302 K). We can use this result as a test of our method—at supersaturations lower than this measured transition, the calculated ΔG_c for {110} should be greater than $3RT$, and at higher supersaturation the opposite should be true.

An attachment energy calculation of biphenyl was performed (Winn, in press) conforming to the previous biphenyl modeling of Docherty and Roberts (1988b). (The two simulations differ in that we employed the DREIDING force field (Mayo et al., 1990), and assumed only dispersive interactions, that is, no coulombic forces.) The three bonds that meet the stable edge criteria are listed in Table 6, and the likely faces are listed in Table 7. Using $\gamma^{solv} = 28.5$ erg/cm^2 for toluene (Kaelble 1971), and, assuming it is completely nonpolar, the kink and edge free energies were calculated.

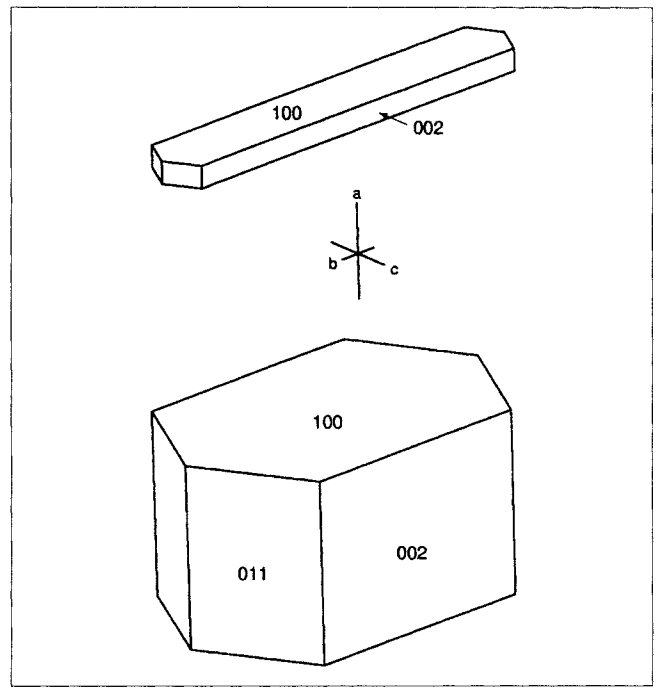

Figure 6. Predicted morphology of ibuprofen crystals grown from hexane (top) and ethanol (bottom).

Hexane grown shape assumes the unstable growth in the b direction is an order of magnitude faster than the slow growth directions.

Table 6. Estimated Interfacial Properties for Biphenyl Crystals in Toluene

Label	ϕ^{cryst} (kJ/mol)	l (Å)	γ^{cryst} (erg/cm^2)	γ^{kink} (erg/cm^2)	ϕ^{kink} (kJ/mol)
i, i^*	11.157	4.94	43.83	1.36	0.36
j	8.516	5.63	38.46	0.53	0.12

Two values of ΔG_c are presented: one calculated at a relative supersaturation of 0.0065, and the other at 0.007. Since $3RT$ is about 7.5 kJ/mol, the lower supersaturation leads to a flat growth on {110} ($\Delta G_c = 7.9$ kJ/mol), while the higher supersaturation results in roughened growth ($\Delta G_c = 7.3$ kJ/mol). We have calculated a precise transition at a relative supersaturation of 0.0069. Thus, our criteria for kinetic roughening and our method for predicting γ^{edge} and ΔG_c predict a roughening transition on {110} that closely matches the experimental result. In addition, the relative growth rates calculated for the flat growth scenario produce a thin lozenge shape (see Figure 7) that matches the experimental morphology (Jetten et al., 1984).

Bennema and co-workers (Jetten et al., 1984; Bennema, 1993) have also presented a method for predicting the roughening of faces. It is based on the theory of Jackson (1958), which predicts thermodynamic roughening, and can also be used to determine qualitatively the faces likely to undergo kinetic roughening. For example, Jetten et al. (1984) predicted that {110} is a likely candidate for kinetic roughening in the above system. Their method is widely viewed as the standard means for predicting roughening transition; the general efficacy of our technique, which for this example was more quantitatively precise, is not yet known.

Conclusion

We have developed a model for predicting the shape of organic crystals under solution growth. It requires only knowledge of pure component properties: the structure and energy of the solid phase—which can be readily calculated by attachment energy calculations—and the surface free energy of the pure solvent. The computational time is minimal, and, thus, it can be used at the early stages of process synthesis.

Table 7. Predicted ΔG_c and Relative Growth Rates for Biphenyl Crystals in Toluene at Two Supersaturations: $\alpha_1 = 0.0065$; $\alpha_2 = 0.007$*

Face	d_{hkl} (Å)	Bond Chains	$\Delta G_c(\alpha_1)$ (kJ/mol)	$R_{rel}(\alpha_1)$	$\Delta G_c(\alpha_2)$ (kJ/mol)	$R_{rel}(\alpha_2)$
001	9.472	i, i^*, j	66.4	1.0	61.6	1.0
110	4.621	i	7.9	8.4	7.3	rough
111	4.239	i				
111	4.072	i				
200	4.044	j	0.9	rough	0.85	rough
201	3.845	j				
201	3.605	j				
112	3.395	j				

*Note the transition to rough growth on {110} with the increased supersaturation.

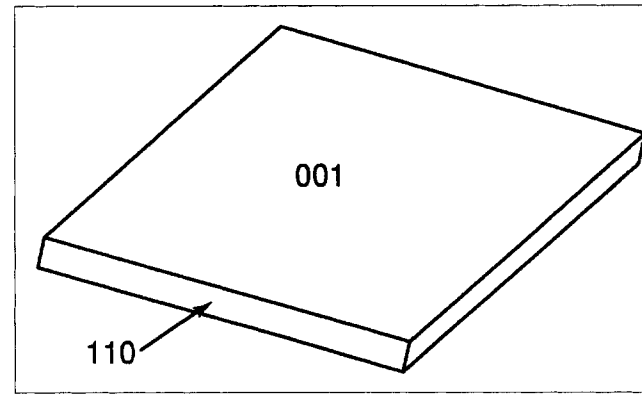

Figure 7. Predicted crystal morphology of biphenyl grown from toluene.

One of the limitations of this approach is that it applies to cases where there are mainly dispersive forces between the solvent and crystal at kinks and steps, or where there are known to be very specific electrostatic interactions (such as water–carboxyl group). The method cannot handle situations where forces are mostly coulombic (such as inorganics) or where there are induced electrostatic interactions between solvent and crystal. Nevertheless, if improved ways of predicting interfacial free energy become available—for example, group contribution methods—then the technique may be able to handle more varied situations. Another, but less important drawback is that it cannot predict the absolute or relative velocities of faces undergoing rough, transport limited growth. However, these fast growing sections are the most susceptible to mechanical abrasion and breakage, and, therefore, even a fully detailed transport model might not result in quantitatively accurate predictions.

The technique uses simplified versions of crystal growth theories. Many of the assumptions, such as the insignificance or isotropy of diffusion (surface or bulk) and steric barriers, have been previously suggested by other authors, and are generally considered reasonable for a first approach. Our criterion for nearest neighbor bonds and stable edges has not been made so explicitly elsewhere. It is one of the critical assumptions of this technique, eliminating many edge directions and faces from consideration, and is by itself a useful tool for determining likely crystal faces. The validity of this assumption will be determined through further application of the model.

Another significant aspect of the model is its potential ability to predict the effects of certain types of additives—surface active agents—on crystal shape. These materials, which are very effective even in small amounts, are increasingly being explored as a means to achieve desired morphological properties. For example, the E. I. DuPont de Nemours Corporation (Klug and van Mil, 1994) have patented a process improvement where they have added a surfactant (sodium dodecyl benzyl sulphonate) to the adipic acid process which results in needle growth along the a axis. (This improves flowability of the suspension by reducing the area of the hydrophilic {100} faces). This surfactant is known to create a hydrocarbon rich surface at the air/water interface, which re-

duces the surface free energy from 70 to 40 erg/cm^2 at room temperature (Porter, (1991). If one presupposes that an equivalent hydrocarbon rich interface forms between the solvent and adipic acid during crystallization, then our model would suggest that bond chains with dispersive forces have small kink free energies, and that only along hydrogen bond chains might there be a large ϕ^{kink}. Thus, flat slow growth should occur only on the {011} and {002} faces, while rough and fast growth should occur along the *a* axis: exactly what is described in the patent. This example suggests that the effect of surface active additives or impurities may be accounted for using this model, when only the properties of the agent in the pure solvent are known.

Acknowledgments

This research was supported by the University of Massachusetts Process Design and Control Center. Special thanks to Professor Klaus Wintermantel and Drs. Matthias Kind, Simon Jones, and Matthias Rauls, who made it possible for one of us (D.W.) to perform the crystallization experiments in the laboratories of BASF AG.

Notation

$A^{\max}_{h,k,l}$ = reticular area of the most dense face intersecting h-bond chains, Å^2/molecule
a, b, c = crystallographic axes
(h,k,l) = crystallographic plane (denotes a crystal face)
$\{h,k,l\}$ = crystal form (family of symmetrically related planes)
$[h,k,l]$ = crystallographic direction
h, i, j = labels of edge directions (bond chains)
D_m = molecular diameter (Å)
ΔG_c = free energy to form a critical 2-D nucleus, kJ or a mole of critical nuclei, kJ/mol
r = radius of a 2-D nucleus (Å)
r_c = radius of a 2-D nucleus of critical size (Å)
R = gas constant, kJ/mol·K
T = temperature, K
V_m = molecular volume, Å^3
y = distance between steps on a crystal face, Å
μ = chemical potential of a solute in solution, kJ/mol
μ^{sat} = chemical potential of a solute in a saturated solution, kJ/mol
Δ_μ = supersaturation: $\Delta\mu = \mu - \mu^{\text{sat}}$, kJ/mol
ϕ^{edge} = work to create an edge on a crystal face, kJ/mol
ϕ^{kink} = work to create a kink in a edge, kJ/mol

Literature Cited

Adamson, A. W., *Physical Chemistry of Surfaces*, Wiley, New York (1990).
Barton, A. F. M., *Handbook of Solubility and Other Cohesive Parameters*, CRC Press, Boca Raton, FL (1983).
Bennema, P., "Growth and Morphology of Crystals," *Handbook of Crystal Growth 1*, D. T. J. Hurle, ed., North-Holland, New York (1993).
Berkovitch-Yellin, Z., "Toward an Ab Initio Derivation of Crystal Morphology," *J. Amer. Chem. Soc.*, **107**, 8239 (1985).
Boek, E. S., W. J. Briels, and D. Feil, "Interfaces between Saturated Aqueous Urea and Crystalline Urea: A Molecular Dynamics Study," *J. Phys. Chem.*, **98**, 1674 (1994).
Bravais, A., *Études Crystallrographiques*, Gauthier-Villars, Paris (1866).
Bunyan, J. M. E., N. Shankland, and D. B. Sheen, "Solvent Effects on the Morphology of Ibuprofen," *Particle Design Via Crystallization*, Ramanarayanan, R. W. Kern, M. Larson and S. Sikdar, eds., Amer. Inst. of Chem. Engs., New York (1991).
Burton, W. K., N. Cabrera, and F. C. Frank, "The Growth of Crystals and the Equilibrium Structure of their Surfaces," *Phil. Trans. Roy. Soc.*, **A243**, 299 (1951).
Cabrera, N., and M. Levine, "On the Dislocation Theory of Evaporation of Crystals," *Phil. Mag.*, **1**, 450 (1956).
Carter, P. W., A. C. Hillier, and M. D. Ward, "Nanoscale Surface Topography and Growth of Molecular Crystals: The Role of Anisotropic Intermolecular Bonding," *J. Amer. Chem. Soc.*, **116**, 944 (1994).
Chernov, A. A., *Modern Crystallography III*, Springer-Verlag, New York (1984).
Chernov, A. A., and T. Nishinaga, "Growth Shapes and Their Stability at Anisotropic Interface Kinetics: Theoretical Aspects for Solution Growth," *Morphology of Crystals, Part A*, I. Sunagawa, ed., Terra Scientific, Tokyo (1987).
Clydesdale, G., R. Docherty, and K. J. Roberts, "HABIT–A Program for Predicting the Morphology of Molecular Crystals," *Comp. Phys. Comm.*, **64**, 311 (1991).
Davey, R. J., "Looking Into Crystal Chemistry," *The Chemical Engineer* (Dec. 1991).
Davey, R. J., S. N. Black, D. Logan, S. J. Maginn, J. E. Fairbrother, and D. J. W. Grant, "Structural and Kinetic Features of Crystal Growth Inhibition: Adipic Acid Growing in the Presence of *n*-Alkanoic Acids," *J. Chem. Soc. Faraday Trans.*, **88**, 3461 (1992).
Docherty, R., and K. J. Roberts, "MORANG–A Computer Program Designed to Aid in the Determination of Crystal Morphology," *Comp. Phys. Comm.*, **51**, 423 (1988a).
Docherty, R. and K. J. Roberts, "Modelling the Morphology of Molecular Crystals; Application to Anthracene, Biphenyl and β-Succinic Acid," *J. Crystal Growth*, **88**, 159 (1988b).
Donnay, J. D. H., and D. Harker, "A New Law of Crystal Morphology Extending the Law of Bravais," *Amer. Min.*, **22**, 446 (1937).
Freidel, M. G., "Études sur la loi de Bravais," *Bull. Soc. Franc. Miner.*, **9**, 326 (1907).
Gavezzotti, A., G. Filippini, J. Kroon, B. P. van Eijck, and P. Klewinghaus, "The Crystal Polymorphism of Tetrolic Acid: A Molecular Dynamics Study of Precursors in Solution, and Crystal Structure Generation," *Chem. Eur. J.*, **3**, 893 (1997).
Giacovazzo, C., "Symmetry in Crystals," *Fundamentals of Crystallography*, C. Giacovazzo, ed., Oxford Univ. Press, Oxford (1992).
Gilmer, G. H., and P. Bennema, "Simulation of Crystal Growth with Surface Diffusion," *J. Appl. Phys.*, **43**, 1347 (1972).
Girifalco, L. A., and R. J. Good, "A Theory for the Estimation of Surface and Interfacial Energies: I. Derivation and Application to Interfacial Tension," *J. Phys. Chem.*, **61**, 904 (1957).
Gordon, R. E., and S. I. Amin, "Crystallization of Ibuprofen," U. S. Patent Number 4,476,248 (1984).
Grant, D. J. W., K. Y. Chow, and H. Chan, "Modification of the Physical Properties of Adipic Acid by Crystallization in the Presence of n-Alkanoic Acids," *Particle Design Via Crystallization*, R. Ramanarayanan, W. Kern, M. Larson and S. Sikdar, eds., AIChE (1991).
Green, D. A., P. Meenan, G. M. Sunshine, and B. J. Enis, "Habit Modelling and Verification for Glutaric Acid," *J. Phys. D.*, **26**, B35 (1993).
Hansen, C., and A. Beerbower, "Solubility Parameters," *Kirk-Othmer Encyclopedia of Chemical Technology*, Wiley, New York (1971).
Hartman, P., and W. G. Perdok, "On the Relations Between Structure and Morphology of Crystals: I," *Acta. Cryst.*, **8**, 49 (1995).
Hildebrand, J. H., and R. L. Scott, *Regular Solutions*, Prentice-Hall, Englewood Cliffs, NJ (1962).
Hoffman, D. W., and J. W. Cahn, "A Vector Thermodynamics for Anisotropic Surfaces," *Surf. Sci.*, **31**, 389 (1972).
Hunan, H. J., J. P. van der Eerden, L. A. M. J. Jetten, and J. G. M. Odekerken, "On the Roughening Transition of Biphenyl: Faceted to Non-Faceted Growth of Biphenyl for Growth from Different Solvents and the Melt," *J. Crystal Growth*, **51**, 589 (1981).
Jackson, K. A., "Mechanism of Growth," *Liquid Metals and Solidification*, Amer. Soc. for Metals, Cleveland (1958).
Jetten, L. A. M. J., H. J. Hunan, P. Bennema, and J. P. van der Eerden, "On the Observation of the Roughening Transition of Organic Crystals Growing from Solution," *J. Crystal Growth*, **68**, 503 (1984).
Kaelble, D. H., *Physical Chemistry of Adhesion*, Wiley-Interscience, New York (1971).
Kaichew, R., "The Molecular-Kinetic Theory of Crystal Growth," *Growth of Crystals*, Vol. 3, A. V. Shubnikov and N. N. Sheftal, eds., Consultants Bureau, New York (1962).

Kitaigorodsky, A. I., *Molecular Crystals and Molecules*, Academic Press, New York (1973).
Klug, D. L., and J. H. van Mil, "Adipic Acid Purification," United States Patent Number 5,296,639 (1994).
Lewis, B., "The Growth of Crystals of Low Supersaturation: I. Theory," *J. Crystal Growth*, **21**, 29 (1974).
Liu, X. Y., and P. Bennema, "The Relationship Between Macroscopic Quantities and the Solid-Fluid Interfacial Structure," *J. Chem. Phys.*, **98**, 5863 (1993).
Liu, X. Y., E. S. Boek, W. J. Briels, and P. Bennema, "Prediction of Crystal Growth Morphology Based on Structural Analysis of the Solid-Fluid Interface," *Nature*, 374, 342 (1995).
Liu, X. Y., and P. Bennema, "Growth Morphology of Crystals and the Influence of Fluid Phase," *Crystal Growth of Organic Materials*, A. S. Myerson, D. A. Green and P. Meenan, eds., ACS, Washington (1996).
Manne, S., J. P. Cleveland, G. D. Stucky, and P. K. Hansma, "Lattice Resolution and Solution Kinetics on Surfaces of Amino Acid Crystals: An Atomic Force Microscopy Study," *J. Crystal Growth*, **130**, 133 (1993).
Markov, I. V., *Crystal Growth for Beginners*, World Scientific, Singapore (1995).
Mayo, S. L., B. D. Olafson, and W. A. Goddard, III, "DREIDING: A Generic Force Field for Molecular Simulations," *J. Phys. Chem.*, **94**, 8897 (1990).
Muller-Krumbhaar, H., "Kinetics of Crystal Growth," *Current Topics in Material Science*, Vol. I, E. Kaldis, ed., North-Holland, Amsterdam (1978).
Myerson, A. S., and R. Ginde, "Crystals, Crystal Growth, and Nucleation," *Handbook of Crystal Growth*, A. S. Myerson, ed., Butterworth-Heinemann, Boston (1993).
Ohara, M., and R. C. Reid, *Modeling Crystal Growth Rates from Solution*, Prentice-Hall, Englewood Cliffs, NJ (1973).
Porter, M. R., *Handbook of Surfactants*, Chapman and Hall, New York (1991).
Saska, M., and A. S. Myerson, "The Theoretical Shape of Sucrose Crystals from Solution," *J. Crystal Growth*, **61**, 546 (1983).
Tanguy, D., and P. Marchal, "Relations between the Properties of Particles and their Process of Manufacture," *Trans. IChemE*, **74**, 715 (1996).
van der Eerden, J. P., "Crystal Growth Mechanisms," *Handbook of Crystal Growth*, D. T. J. Hurle, ed., North-Holland, Amsterdam (1993).
Voronkov, V. V., "Dislocation Mechanism of Growth with a Low Kink Density," *Sov. Phys. Crystallog.*, **18**, 19 (1973).
Wells, A. F., "Crystal Habit and Internal Structure: I," *Phil. Mag.*, **37**, 184 (1946).
Winn, D., "Predicting Crystal Shape in Organic Solids Processes," PhD Thesis, Univ. of Massachusetts, Amherst (in press).
Yip, C. M., and M. D. Ward, "Atomic Force Microscopy of Insulin Single Crystal: Direct Visualization of Molecules and Crystal Growth," *Biophys. J.*, **71**, 1071 (1996).

Appendix

2-D nucleation birth and spread model

The birth and spread model of crystal growth is thought to be the most realistic of the 2-D nucleation growth models (Ohara and Reid, 1973). It is often assumed that the most significant face-dependent variables in this mechanism are the activation energy for desolvation U and the free energy change to form a critical nucleus ΔG_c (Liu and Bennema, 1996). (The latter dictates the equilibrium concentration of critical nuclei.) Using the development of Markov (1995), we can write the expression for relative growth rates as

$$R_{\text{rel}} \propto \exp(-U/RT)\exp(-\Delta G_c/3RT) \tag{33}$$

Molecules attaching to nuclei can either enter into kinks, or adsorb onto flat edges so as to form kinks. Since we apply the 2-D nucleation model when the free energy of kink formation is low, there is likely to be a high density of kinks on any edge: there is a high probability that molecules entering the solid state form kinks. The amount of desolvation of these molecules can be estimated using the *proportionality approximation* (Liu and Bennema, 1996), which assumes that the anisotropy of solute–solvent bonding is proportional to the anisotropy of solid–solid bonding. It can be expressed as

$$\frac{U^{\text{sl}}}{U^{\text{tot}}} = \frac{E^{\text{sl}}}{E^{\text{latt}}} \tag{34}$$

and

$$\frac{U^{\text{att}}}{U^{\text{tot}}} = \frac{E^{\text{att}}}{E^{\text{latt}}} \tag{35}$$

where U^{sl} is the amount of energy (kJ/mol) to desolvate the portion of the molecule that is parallel to the crystal face (lateral interactions), and U^{att} is the amount to desolvate the molecule in the direction orthogonal to the crystal face (kJ/mol). The sum of the two are constant and equal to U^{tot}. The symbols E^{sl} and E^{att} are the slice and attachment energies (kJ/mol), analogous properties that refer to the solid–solid bonding in the crystal (see Hartman and Perdok, 1955, for details). Their sum is equal to the lattice energy E^{latt} (kJ/mol) which is a constant.

For a simple cubic crystal lattice, a molecule adsorbing onto an edge must lose one-half of its orthogonal interactions with the solvent and one-quarter of its lateral interactions with the solvent. We can express the desolvation energy as

$$\begin{aligned} U &= U^{\text{sl}}/4 + U^{\text{att}}/2 \\ &= \left(\frac{E^{\text{sl}}/4 + E^{\text{att}}/2}{E^{\text{latt}}}\right) U^{\text{tot}} \\ &= \left(1/2 - \frac{E^{\text{sl}}/4}{E^{\text{latt}}}\right) U^{\text{tot}} \end{aligned} \tag{36}$$

Therefore, the greater the slice energy of a face, the smaller the desolvation energy. The total desolvation energy is approximately the difference between the sublimation enthalpy and the dissolution enthalpy ($U^{\text{tot}} \approx \Delta H_{\text{sub}} - \Delta H_{\text{diss}}$, which implies $U^{\text{tot}} \sim 10$ to 100 kJ/mol), and thus U has the same order of magnitude as ΔG_c for organics in solution.

We also know that the greater the slice energy, the greater the magnitude of unsaturated interactions at the edges, and the greater the value of γ^{edge}. Since ΔG_c increases with the square of γ^{edge}, it is expected that ΔG_c increases more rapidly than U decreases. Therefore, the relative growth rates should still decrease as ΔG_c increases, but not at an exponential rate. We, therefore, propose the following expression for the relative growth rate for growth by 2-D nucleation

$$R_{\text{rel}} \propto 1/\Delta G_c \tag{37}$$

Equation 37 simplifies the growth model of Eq. 33 and Eq. 36 and provides good morphological predictions.

Spiral growth model

In the spiral growth model, the desolvation step is also part of the complete growth mechanism. However, the spiral mechanism is applied when kink free energies are high and kink densities are low, and, thus, most solute molecules are assumed to be incorporating into kink sites (as opposed to making kink sites). A molecule entering into a kink position forms, on average, half of its total solid–solid bonds: half of the orthogonal interactions, and half of the lateral interactions. (In the simple cubic lattice, this is exactly true). Using the proportionality approximation, we can again estimate the desolvation energy

$$U = \left(\frac{(E^{\text{att}}/2 + E^{\text{sl}}/2)}{E^{\text{latt}}} \right) U^{\text{tot}}$$
$$= U^{\text{tot}}/2 \tag{38}$$

Therefore, the desolvation energy for entering a kink is isotropic, and we need not include the desolvation step in the relative growth rate expressions for spiral growth.

Manuscript received May 18, 1998, and revision received Sept. 3, 1998.